inter.noise
27-30 AUGUST HONG KONG 2017

The sonAIR aircraft noise simulation tool

Jean Marc WUNDERLI[1], Christoph ZELLMANN[1], Micha KÖPFLI[2]; Olivier SCHWAB[1], Felix SCHLATTER[1], Beat SCHÄFFER[1]

[1] Empa, Laboratory for Acoustics/Noise Control, Dübendorf, Switzerland

[2] n-Sphere AG, Zürich, Switzerland

ABSTRACT

The aircraft noise simulation model sonAIR has been designed to precisely predict single flights with the scope to investigate and optimize noise abatement procedures. With its current implementation it is also possible to do noise mapping for entire airports. The simulation process is based on a time-step approach in which single flights are represented in a high temporal resolution. Several sound source models are available, from detailed models for turbofan powered aircraft, which describe airframe and engine noise separately with a three dimensional directivity pattern, to simplified models for a wide variety of propeller driven aircraft and helicopters. An advanced sound propagation model is used, which for example pays particular attention to air attenuation through a stratified atmosphere. The whole simulation chain is formulated for one-third-octave-bands, within a frequency range of 25 Hz to 5 kHz. The full implementation of the program in a geographical information system (GIS) allows for a user-friendly calculation process. In this contribution an overview of the calculation process is given and first results of model verifications as well as application examples are presented.

Keywords: Aircraft, Noise, Modelling, Mapping I-INCE Classification of Subjects Number(s): 13 / 24

1. INTRODUCTION

The ICAO *Balanced Approach to Aircraft Noise Management* (1), addresses the aircraft noise problem with four principal elements: (a) reduction of noise at source, (b) land-use planning and management, (c) noise abatement operational procedures and (d) operation restrictions on aircraft. For the implementation of the Balanced Approach as well as for legal compliance issues, aircraft noise simulation tools play a crucial role. These tools on the one hand have to fulfill high requirements in terms of reliability, accuracy and credibility. On the other hand, they should have the flexibility to account for the effects of different take-off and landing procedures, as proposed by ICAO in (c) as one of the primary mitigation measures for aircraft noise. In addition, the computational demand should be such as to allow noise mapping for wide areas of several 1'000 km^2 in combination with a large number of simulated flights.

To date, several approaches exist with various levels of sophistication to calculate aircraft noise (2). A widely used approach is described by ECAC Doc.29 (3) or its equivalent, ICAO Doc.9911 (4). The method is used to assess aircraft noise impact in the US (required by the Federal Register) and for strategic noise mapping in Europe (Environmental Noise Directive 2002/49/EC (5)). Current implementations are AEDT (6) and IMPACT (7) with the scope to assess the environmental impact on a local scale (single flights, airports) as well as on a global scale (national and beyond). Again both tools base on Doc.29 / Doc.9911. In addition, several tools for the detailed prediction of the noise of single flights are developed that rely on semi-empirical models for single sound sources. These models were first implemented in ANOPP (8) but are also used for low-noise aircraft design in PANAM (9). Other programs such as SIMUL (10) feature detailed, semi-empirical models with partial sound sources, that have been derived based on extensive measurements. A drawback of this approach is that emission data is only available for a small set of aircraft.

While the Doc. 29 / Doc. 9911 implementations are suitable for the calculation of whole scenarios,

[1] Jean-Marc.Wunderli@empa.ch

they are of limited applicability for the prediction of the noise of single aircraft events (11). First, they do not account for the effects of airspeed or aircraft configuration, despite their particular importance for approach procedures. Second, the spectral description is based on spectral classes at the maximum momentary level, which leads to uncertainties of the attenuations at larger distances. These shortcomings are no issue for the semi-empirical tools described above (8-10), which predict spectra and directivity for each source on a high level of detail. However, they either require very detailed input data of the geometry of the sources (e.g. gear dimensions) as well as of the flight parameters (e.g. primary jet speed, airflow mass) for accurate predictions or they are only available for a small set of aircraft. Also, these tools are not publicly available.

The sonAIR aircraft noise model was developed to overcome some of these limitations and to provide a reliable prediction tool for noise abatement operational procedures which is still applicable for noise mapping. Particular attention was thereby given to a high level of flexibility, allowing for calculations with different levels of detail of the input parameters. This paper shortly introduces the concept of sonAIR, but primarily focusses on verification and application examples, which underline the model accuracy and flexibility in use.

2. The sonAIR simulation tool

The sonAIR simulation model, consisting of a sound source and a propagation model, is formulated for one-third-octave-bands, within a frequency range of 25 Hz to 5 kHz.

2.1 Sound source model

During the initial project phase of sonAIR from 2012 to 2016 a sound source model was developed based on a multiple regression approach and, a methodology was derived to separate engine noise from airframe noise. In an extensive acoustic measurement campaign of real air traffic at Zurich airport a total of 2'600 overflights in the close range of the airport, each recorded at eight different microphone locations, and 11'000 overflights in the far range of the airport at three to four different locations per flight were recorded. On that basis, sound source models were derived for the 19 turbofan powered aircraft given in Table 1, covering the majority of commercial aircraft operating in Switzerland. For six aircraft types in Table 1 flight data records (FDR) provided by SWISS International Airlines were available. On that basis, detailed models (referred to as 3D in the following account) in dependence of the aircraft configuration could be derived. For the 13 other aircraft types, reduced models without configuration (3Dred) were established.

Both model types separately predict engine and airframe noise. The engine noise model exhibits a three-dimensional directivity pattern in dependence of the rotational speed of the low pressure compressor *N1* in % as input parameter. Airframe noise models for aircraft type with FDR data (3D) predict a two-dimensional directivity pattern in dependence of the configuration, Mach number and air density as inputs. The reduced airframe noise models (3Dred) neglect the influence of configuration. All airframe noise models feature a two dimensional directivity pattern. For more details on the sonAIR sound source models for turbofan powered aircraft it is referred to (12).

Table 1 – sonAIR sound source models (3D with aircraft configuration and 3Dred without) for turbofan powered aircraft and the number of overflight events.

Aircraft type	Engine type	Model	Dep.	Appr.	Total
Airbus A319-100	CFM56-5B	3D	120	41	161
Airbus A320-200	CFM56-5B	3D	424	249	673
Airbus A321-200	CFM56-5B	3D	300	126	426
Airbus A320-Family	CFM56-5A	3Dred	57	15	72
Airbus A320-Family	V2500	3Dred	198	33	231
Airbus A330-300	TRENT7	3D	249	136	385
Airbus A340-300	CFM56-5C	3D	166	120	286
Airbus A380-800	GP7270	3Dred	26	2	28
Airbus A380-800	TRENT9	3Dred	38	20	58
Boeing B737 Classic (-300 to -500)	CFM56-3	3Dred	84	39	123
Boeing B737 NG (-600 to -900)	CFM56-7B	3Dred	297	37	334
Boeing 767-300	PW4060	3Dred	9	34	43
Boeing 767-Family (-200 to -400)	CF6-80C2	3Dred	19	57	76
Bombardier Regional Jet CRJ-900	CF34-8C5	3Dred	71	22	93
Embraer ERJ 170	CF34-8E	3Dred	62	27	89
Embraer ERJ 190	CF34-10E	3Dred	243	49	292
Fokker 100	TAY650-15	3Dred	234	61	295
Dassault Falcon 7X	PW307	3Dred	17	10	27
BAE SYSTEMS AVRO RJ-100	LF507	3D	324	202	526

The above database does not cover the wide variety of aircraft operating in Switzerland or other countries. Therefore, as a complement to the existing data base, an interface has been established to the Swiss Aircraft Noise Calculation Database (SANC-DB), which is maintained by the Federal Office of Civil Aviation (FOCA) and comprises sound emission data of all noise certified aircraft in Switzerland, in total over 1'500 wing-mounted aircraft (commercial and general aviation), military jets and helicopters (13, 14). In addition an open standard for sound emission data given as look-up tables has been defined, which allows the integration of external source models.

2.2 Propagation model

sonAIR is part of a family of noise calculation models, which today consists of models for road traffic noise (sonROAD (15)), railway noise (sonRAIL (16, 17)) and shooting noise (sonARMS (18)). As the physics of sound propagation is in principal independent of the type of sound source, they all rely on the same propagation core, called sonX. However, depending on the sound source, the propagation situation, the envisaged accuracy and the available computational power, simplifications may be appropriate in some cases. As an example, lateral sound paths around barriers can have a major effect for stationary point sources and are therefore taken into account for shooting noise. But those sound paths are neglected for traffic noise, where the moving point sources automatically create an averaging in the horizontal plane. Consequently the sonX propagation model is formulated with a modular structure and allows activating refinements if intended.

The sonX propagation model is formulated for point sources, accounting for the corresponding laws of geometrical spreading. In the sound propagation model contributions from direct sound as well as three types of reflections are calculated separately: (a) a model for reflections at buildings, walls and other rigid surfaces (19, 20), (b) a model for diffuse sound reflections at forests (21) and (c) a model for reflections at cliffs (22). However, as reflections are typically not taken into account for aircraft noise, these models are only used in exceptional cases.

Direct sound can either be calculated under the assumption of a homogenous atmosphere or based on vertical profiles of temperature, relative humidity, air pressure and wind speed. In the latter case, the atmosphere is stratified in sections of 100 m height, and representative air absorption coefficients per one-third-octave-band are calculated for each section and summed up. Information on a detailed analysis of the influence of air absorption under varying weather conditions with a stratified

atmosphere can be found in (23). For gracing sound incidence a ray tracing algorithm is applied, which accounts for meteorological influences on shielding effects. In combination with an empirical extension also sound exposure level in acoustical shadow zones are predicted (24).

2.3 Calculation procedure

For the simulation of aircraft noise, a time-step method is applied. Single flights are represented in a temporal resolution of usually one second with the current position and orientation as well as thrust setting and configuration as input parameters. This approach allows a detailed analysis of the sound exposure at any point of interest, yielding not only spectral information but also level-time histories.

For each source and receiver combination, the sound emission level $\hat{L}_{em}(f,\theta,\varphi)$ is calculated in dependency of the frequency and the radiation angles θ, φ, to derive the sound pressure level Leq according to Equation (1). Therefore, the flight track also needs to provide the model dependent flight parameters in a fine temporal resolution.

$$Leq_j(f) = \hat{L}_{em,j}(f,\theta,\varphi) + \Delta L_{FE,j} - \sum A_j(f) \tag{1}$$

with Leq as the sound pressure level at receiver [dB], $\hat{L}_{em}$ as the sound emission level [dB], ΔL_{FE} as the flight effect [dB], $\sum A$ as the sum of attenuations [dB], and j as the index of the source position.

The flight effect ΔL_{FE} as given in Equation 2 according to (25) accounts for the kinematic effect. The latter corresponds to the motion of the source relative to the receiver as well as the dynamic effect which accounts for the motion of the source relative to the propagation medium (26).

$$\Delta L_{FE,j} = 40 \cdot \log_{10}\left(\frac{1}{1 - Ma_j \cdot \cos\theta_j}\right) \tag{2}$$

with θ as the longitudinal radiation angle [°] and Ma as the Mach number [-].

Based on the $Leq_j(f)$, A-weighted level-time histories are calculated to derive the event level L_{AE} and the maximum level $L_{AS,max}$ for each receiver. In principle, arbitrary weightings as well as different metrics based on one-third-octave bands can be calculated.

For the task of noise mapping, calculations are performed for a receiver grid with a constant height above ground. In aircraft noise simulation typically numerous single flights are processed together resulting in a so-called footprint, i.e., the sound exposure of an averaged single flight of a bundle of flights, on all receiver points arranged in a grid. As input either radar tracks of a distinct combination of aircraft and route, or idealized tracks with several off-set routes are used (27). As a last step, these footprints are weighted with the number of movements per aircraft and route and the contributions from all aircraft and route combinations are energetically summed up. Based on these results, comparisons with noise limits or statistics on the number of affected people (e.g. high annoyance, sleep disturbance) can be derived.

2.4 Simulation tool

The sonAIR simulation model has been implemented in a geographic information system (GIS) on the Esri ArcGIS basis. This platform provides helpful tools for importing, visualizing and editing georeferenced information and is prepared for the management of vast databases. Apart from air traffic data, information on topography, land-use types and, if desired, building layers are processed. The calculation process is optimized by implementing a multi-client system, which distributes calculation tasks to several nodes, monitors the calculation process, and collects and combines the results. Additional benefits of the implementation are user-friendly reporting tools and a data management system, which provides a central data storage and allows holding different states and scenarios. In addition to noise maps, also further analysis of affected people or areas is possible.

3. Model verification and examples of application

3.1 Model verification

So far only measurement data is available which was used for the model fitting. Therefore a real validation of the model with external data is still pending. Consequently in this section only a model

verification can be shown, i.e. how accurately the measurements can be reproduced by calculations. A scatter plot in Figure 2 (left) compares the simulated event levels of the advanced 3D model with the measured event levels L_{AE}. In total 10'524 measurements for six aircraft types with available FDR data are compared. In general, the calculated L_{AE} correlate well with the measurements, all data scatter symmetrically along the 1:1 line. An exception is found for L_{AE} below 80 dB. Here, the simulated values tend to overestimate the measured L_{AE}. Between approach and departure no obvious differences in the variance or in the correlation with measurements are detected.

In Figure 2 (right) overall 5'278 measurements for 13 aircraft types without FDR data were simulated (3Dred) and compared to measurements. The event levels agree similarly well with the measurements for the whole level range as for the types with FDR data. In contrast to the 3D models, however, the standard deviation for approach is slightly larger than for departures, which can be explained by the reduced level of detail of the model without configuration. Nevertheless the accuracy is very good, despite the missing information on aircraft configuration: This can be explained by the fact that the configuration is highly correlated with speed and thus indirectly represented in the reduced models.

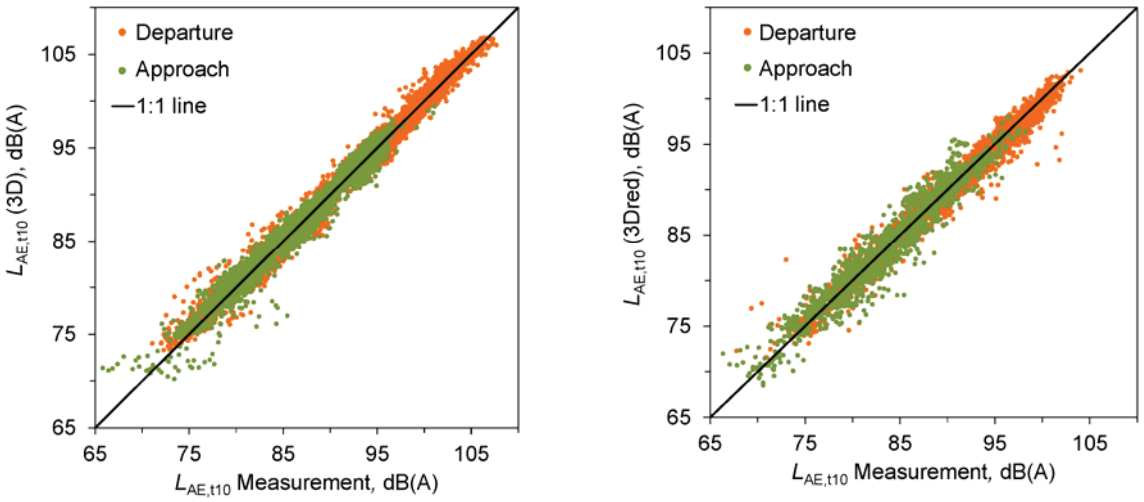

Figure 2 – Comparison between measured $L_{AE,t10}$ and the 3D model for types with FDR data (left) and the 3Dred model for types without FDR data (right).

The statistical analysis of the comparison between calculations and measurements reveals that the mean difference of $\Delta L_{AE,t10}$ (calculation minus measurement) for the 3D models with 0.1 dB is small and the measurements of the six types with FDR data are reproduced adequately (

Table 1). The standard deviation amounts to 0.9 dB. The mean of $\Delta L_{AE,t10}$ for the 13 types without FDR data (3Dred) is zero, but the standard deviation is with 1.2 dB larger than for 3D.

Table 1 – Level differences in dB ($\Delta L_{AE,t10}$, calculation minus measurement) of six types with 3D model (based on 10'524 events) and 13 types with 3Dred (based on 5'278 events).

Model	**Mean**	Standard dev.	Max.	Min.	p-value
3D (6 types)	**0.1**	0.9	5.6	−8.5	< 0.01
3Dred (13 types)	**0.0**	1.2	9.3	−8.5	0.86

3.2 Level-time histories

Figure 3 shows level-time histories for two departures of an A340-300 from runway 16 at Zurich airport. On the left side the actual take-off mass (ATOM) of the aircraft is low with 195 t compared to 268 t on the right side. The low ATOM allows the pilot to reduce the take-off power to $N1 = 87\%$ compared to $N1 = 97\%$, which was required for the departure with a large ATOM. The calculated level-time histories are in very good agreement with the measurements, which were performed closely behind the runway. The measured $L_{AE,t10}$ of 98.6 dB(A) and 107.2 dB(A) were slightly underestimated with the simulation by 0.5 dB.

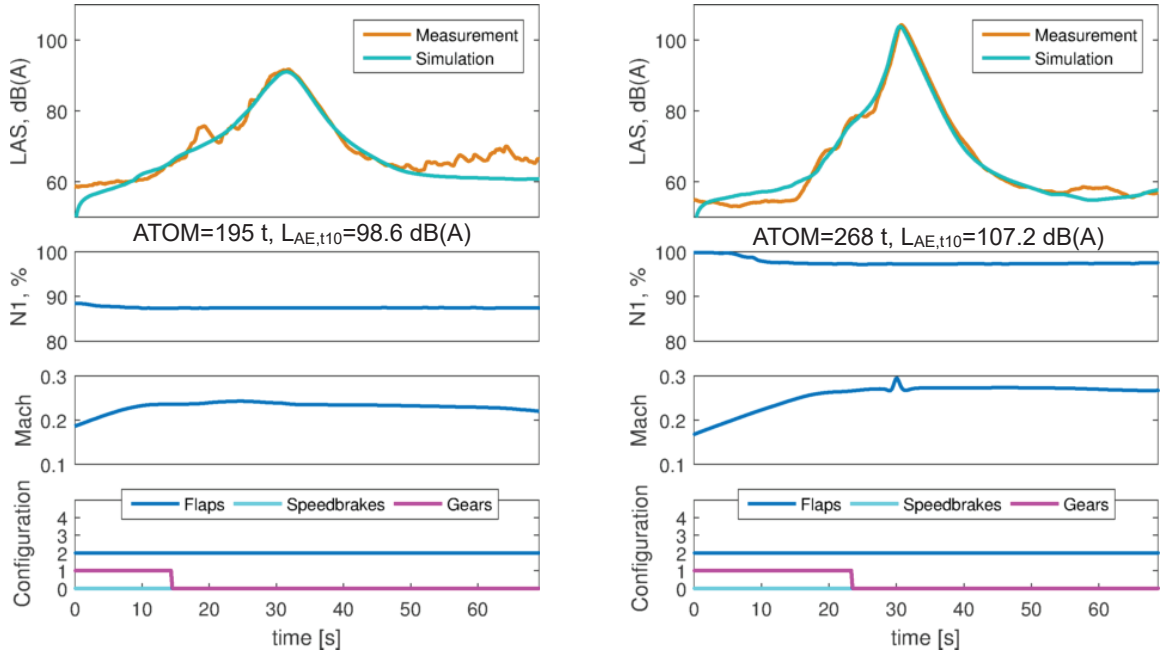

Figure 3 – Level time histories and model parameters for a departure of a A340-300 with low take-off power setting (left) and high take-off power (right). The microphone was located 400 m in extension of runway 16.

One reason for the level difference of 8.6 dB between both departures is the closest distance to the receiver, which was three times higher for the departure with low ATOM. For a line source a factor of three in distance corresponds to 4.8 dB, which is accounted for by the atmospheric divergence in the simulation. In addition, the sound source model accounts for the change of *N1* with a difference between both sound emission levels of approximately 4 dB. Thus the altered power setting accurately accounts for the changes of the sound emission level of the aircraft. In combination with the increased propagation distance, the measured level difference of 8.6 dB can be explained.

3.3 Static and dynamic noise mapping

In the same manner as the calculation of $L_{AE,t10}$ or $L_{AS,max}$ for a single receiver as presented above, entire grids are calculated resulting in acoustic footprints. The latter can later be used to calculate entire noise maps, based on the corresponding number of events per aircraft and route. Figure 4 shows such an acoustic footprint of a single flight as a noise map with contour lines. Several propagation effects are visible, such as the influence of topography, which causes local level variations due to ground reflections and shielding effects. Foliage attenuation of a forest, which lies in parallel to the runway, leads to a significant decrease of noise contours. In addition, a change of the sound emission level can be found at the cutback, where *N1* is considerably reduced.

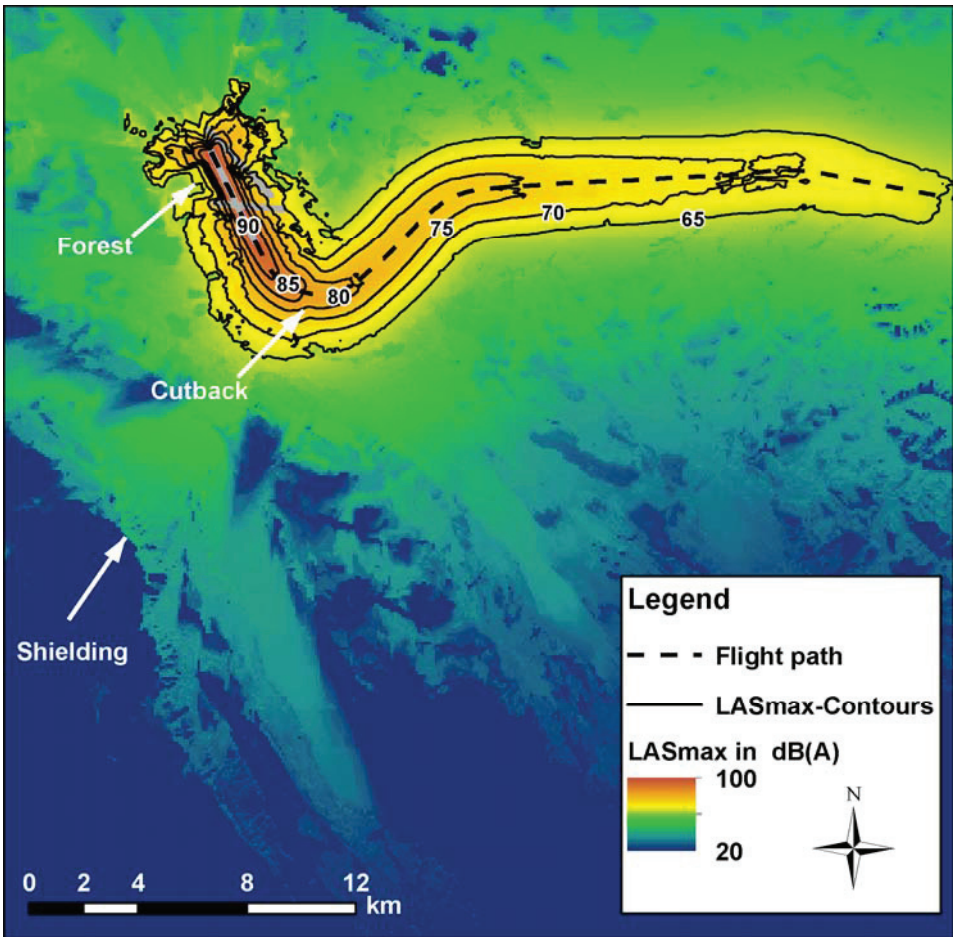

Figure 4 – Example of an acoustic footprint of a single flight, a take-off of an Airbus A330-300 from runway 16 of Zurich airport.

As a consequence of the time-step procedure of single flights, it is not only possible to produce static noise maps. Figure 5 shows a snapshot of a dynamic sound level map of the same flight event with the momentary sound pressure level depicted.

In combination with information on the population distribution, the number of affected persons can be studied, as exemplarily shown in Figure 6. The heat map has thereby been calculated with a linearly increasing weight from 0 to 1 for inhabitants between 50 and 70 dB(A). Inhabitants below 50 dB(A) are not counted and inhabitants above 70 dB(A) got a full weight. Such dynamic maps on the one hand allow studying distinct source as well as propagation effects. On the other hand these visualizations can be used for communication purposes.

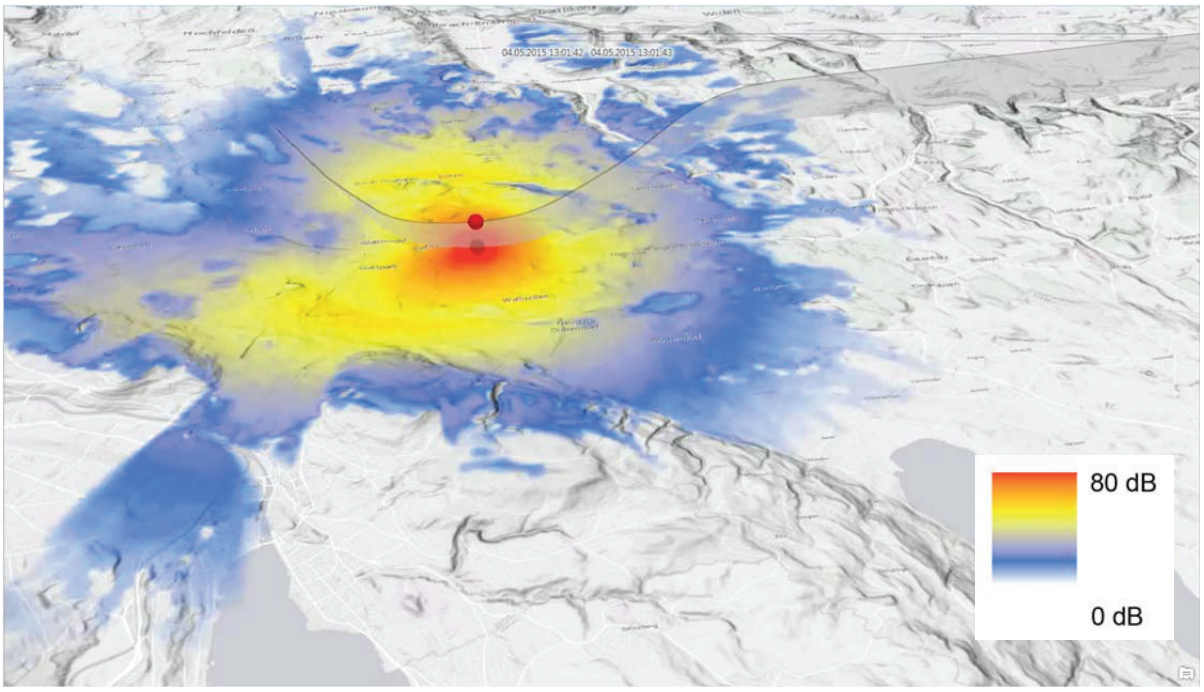

Figure 5 – Example of a dynamic noise map showing the momentary sound pressure level of the same flight as depicted in Figure 4.

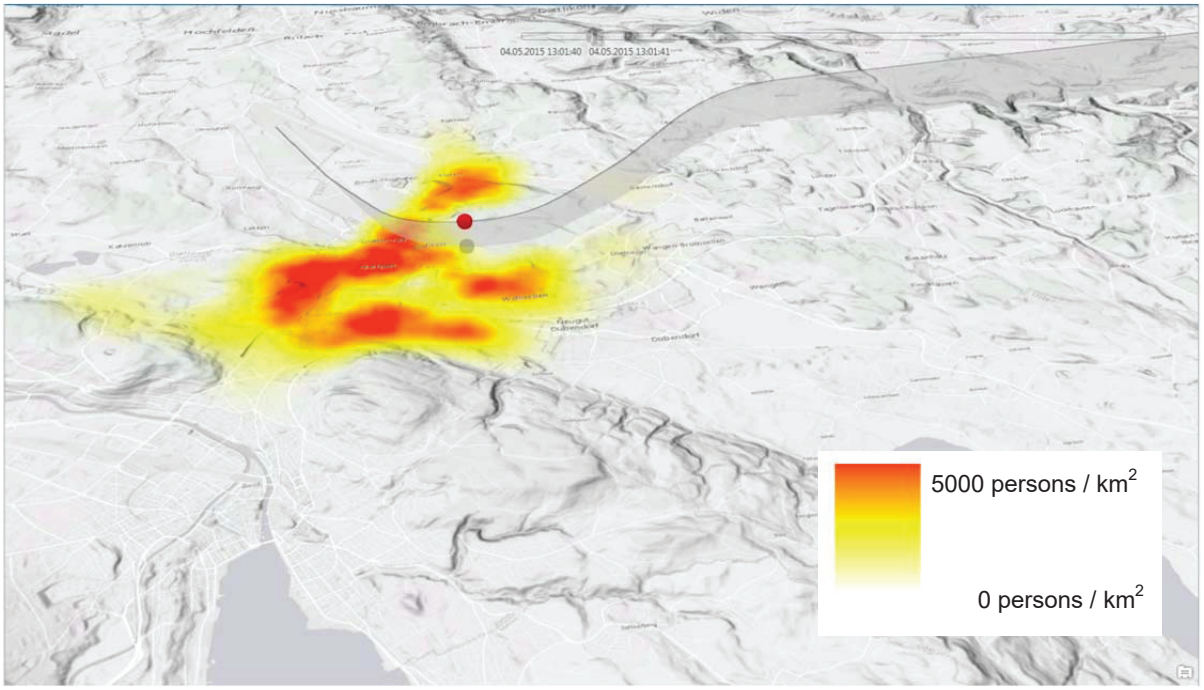

Figure 6 – Example of a dynamic noise map showing the number of affected people for the situation shown in Figure 5.

4. CONCLUSIONS AND OUTLOOK

The recently established aircraft noise model sonAIR with its implementation as a simulation tool allows analyzing not only single flights in great detail, but also entire airport scenarios. The detailed sound source models in combination with a flexible and highly detailed propagation model offer great potential for comparing the effects of different take-off and landing procedures, thus responding to ICAO's Balanced Approach. It is the intention to use sonAIR as a key element in the optimization of air traffic with the goal of reducing the noise burden around airports. As next steps in the development of the tool, a model validation with external data and an extension of the sound source database are planned. For further information about the model and its availability for other users please contact the authors of this contribution.

ACKNOWLEDGEMENTS

The project sonAIR was funded by the Swiss Federal Office of Civil Aviation (FOCA), Empa, skyguide, the Office of Transport of the canton of Zurich as well as by Zurich and Geneva airports. The development of the sound propagation and the implementation of sonAIR in a geographical information system have been financed by the Swiss Federal Office for the Environment (FOEN). The authors would also like to thank SWISS International Airlines for their support.

REFERENCES

1. ICAO. Guidance on the Balanced Approach to Aircraft Noise Management. Doc 9829 AN/451. Montreal (Canada); 2008. Report No.: Doc 9829 AN/451.
2. Bütikofer R. Concepts of aircraft noise calculations. Acta Acust Acust. 2007;93(2):253-62.
3. ECAC. DOC.29: Report on Standard Method of Computing Noise Contours around Civil Airports, Volume 2: Technical Guide. 4th ed. Neuilly-sur-Seine, France: European Civil Aviation Conference (ECAC); 2016 7.12.2016. Available from: https://www.ecac-ceac.org/ecac-doc-29 (last viewed on 01/02/2017).
4. ICAO. Recommended Method for Computing Noise Contours Around Airports. Doc 9911. Montreal (Canada); 2008.
5. EU. DIRECTIVE 2002/49/EC OF THE EUROPEAN PARLIAMENT AND OF THE COUNCIL of 25 June 2002 relating to the assessment and management of environmental noise. Official Journal of the European Communities; 2002. Available from: http://ec.europa.eu/environment/noise/directive_en.htm.
6. Ahearn M, Boeker E, Gorshkov S, Hansen A, Hwang S, Koopmann J, et al. Aviation Environmental Design Tool (AEDT), Technical Manual, Version 2b. 2016 03.05.2016.
7. EUROCONTROL. IMPACT: Impact assessments for noise, gaseous and particulate emissions, and local air quality.; 2016. Available from: http://www.eurocontrol.int/services/impact.
8. Kontos KB, Janardan BA, Gliebe PR. Improved NASA-ANOPP Noise Prediction Computer Code for Advanced Subsonic Propulsion Systems. Volume 1: ANOPP Evaluation and Fan Noise Model. 1996.
9. Bertsch L, Dobrzynski W, Guerin S. Tool Development for Low-Noise Aircraft Design. J Aircr. 2010;47(2):694-9.
10. Bertsch L, Isermann U. Noise prediction toolbox used by the DLR aircraft noise working group. 42nd International Congress and Exposition on Noise Control Engineering 2013, INTER-NOISE 2013: Noise Control for Quality of Life 2013.
11. Schäffer B, Zellmann C, Krebs W, Plüss S, Eggenschwiler K, Bütikofer R, et al. Sound source data for aircraft noise calculations: state of the art and future challenges. Euronoise 10-13 June 2012; Prag 2012. p. 589-94.
12. Zellmann C, Wunderli JM, Paschereit CO. The sonAIR sound source model: spectral three-dimensional directivity patterns in dependency of the flight condition. INTER-NOISE; Hamburg (Germany) 2016.
13. BAFU, BAZL, GS-VBS. Leitfaden Fluglärm, Vorgaben für die Lärmermittlung. Umwelt-Vollzug, Lärm Nr. 1625. Bern, Switzerland: Bundesamt für Umwelt (BAFU), Bundesamt für Zivilluftfahrt (BAZL), Generalsekretariat des Eidg. Departementes für Verteidigung, Bevölkerungsschutz und Sport VBS (GS VBS); 2016. Available from: www.bafu.admin.ch/fluglaerm-ermittlung (zuletzt besucht: 30.09.2016).
14. Krebs W, Lobsiger E. Swiss Aircraft Noise Calculation Database, Technical Documentation, Version 2.0. Empa Laboratory for Acoustics/Noise Control, Swiss Federal Laboratories for Material Science and Technology, Duebendorf, Switzerland; 2012 2012-04-24.
15. Heutschi K. SonRoad: New Swiss road traffic noise model. Acta Acust Acust. 2004;90(3):548-54.
16. Thron T, Hecht M. The sonRAIL emission model for railway noise in Switzerland. Acta Acust Acust.

2010;96:873-83.
17. Wunderli JM. sonRAIL - From the scientific model to an application in practice. Euronoise; Prague 2012. p. 475-80.
18. Wunderli JM, Pieren R, Heutschi K. The Swiss shooting sound calculation model sonARMS. NCEJ. 2012;60(3):224-35.
19. Heutschi K. Calculation of Reflections in an Urban Environment. Acta Acust Acust. 2009;95(4):644-52.
20. Heutschi K. Incoherence Factor as Descriptor for the Diffusivity of Building Facades. Acta Acust Acust. 2011;97:933-9.
21. Wunderli JM. An extended model to predict reflections from forests. Acta Acust Acust. 2012;98(2):263-78.
22. Pieren R, Wunderli JM. A Model to Predict Sound Reflections from Cliffs. Acta Acust Acust. 2011;97(2):243-53.
23. Zellmann C, Wunderli JM. Influence of the atmospheric stratification on the sound propagation of single flights. INTER-NOISE; Melbourne, Australia 2014.
24. Hofmann J, Heutschi K. An engineering model for sound pressure in shadow zones based on numerical simulations. Acta Acust Acust. 2005;91(4):661-70.
25. Merriman J, Good R, Low J, Yee P, Blankenship GL. Forward motion and installation effects on engine noise. In: Astronautics AIoAa, editor. 3rd Aeroacoustics Conference 1976.
26. Stone JR. Flight effects on exhaust noise for turbojet and turbofan engines - comparison of experimental data with prediction. J Acoust Soc Am. 1976;60:113.
27. Schäffer B, Bütikofer R, Plüss S, Thomann G. Aircraft noise: accounting for changes in air traffic with time of day. J Acoust Soc Am. 2011;129(1):185-99.